Huertas-Tato, J., Aler, R., Galván, I.M., Rodríguez-Benítez, F.J., Arbizu-Barrena, C., Pozo-Vázquez, D. (2020).A short-term solar radiation forecasting system for the Iberian Peninsula. Part 2: Model blending approaches based on machine learning. *Solar energy*, 195, pp. 685-696.

DOI: 10.1016/j.solener.2019.11.091

A short-term solar radiation forecasting system for the Iberian Peninsula. Part 2: Model blending approaches based on machine learning

Javier Huertas-Tato[a], Ricardo Aler[a,*], Inés M. Galván[a], Francisco J. Rodríguez-Benítez[b], Clara Arbizu-Barrena[b], David Pozo-Vázquez[b]

[a] EVANNAI Res. Group, Department of Computing Science, Univ. Carlos III, 28911 Madrid, Spain
[b] MATRAS Res. Group, Department of Physic, University of Jaén, 23071 Jaén, Spain

ARTICLE INFO

Keywords:
GHI
DNI
Blending
Machine learning
Regional forecast

ABSTRACT

In this article we explore the blending of the four models (Satellite, WRF-Solar, Smart Persistence and CIADCast) studied in Part 1 by means of Support Vector Machines with the aim of improving GHI and DNI forecasts. Two blending approaches that use the four models as predictors have been studied: the horizon approach constructs a different blending model for each forecast horizon, while the general approach trains a single model valid for all horizons. The influence on the blending models of adding information about weather types is also studied. The approaches have been evaluated in the same four Iberian Peninsula stations of Part 1. Blending approaches have been extended to a regional context with the goal of obtaining improved regional forecasts. In general, results show that blending greatly outperforms the individual predictors, with no large differences between the blending approaches themselves. Horizon approaches were more suitable to minimize rRMSE and general ap-proaches work better for rMAE. The relative improvement in rRMSE obtained by model blending was up to 17%for GHI (16% for DNI), and up to 15% for rMAE. Similar improvements were observed for the regional forecast. An analysis of performance depending on the horizon shows that while the advantage of blending for GHI remains more or less constant along horizons, it tends to increase with horizon for DNI, with the largest im-provements occurring at 6 h. The knowledge of weather conditions helped to slightly improve further the forecasts (up to 3%), but only at some locations and for rRMSE.

1. Introduction

In the companion paper (Part 1), four different short term solar (GHI and DNI) forecasting models (Satellite based model, WRF Solar, Smart Persistence and CIADCast) were presented and their performance was evaluated at four stations located in the Iberian Peninsula. Results showed that those models are complementary because no model out performs the rest for all forecasting horizon, location or variable (GHI and DNI).

In this second part we aim to explore the benefits obtained by de veloping optimal integration (blending) models, using Machine Learning techniques. The question arises of whether an optimal blending of the four models can provide enhanced forecasts at any forecasting horizon and station compared with the most accurate forecasts derived from a single model, taking advantage of their sy nergies and complementarities (Vislocky and Fritsch, 1995). This question is not new in the framework of weather forecasting research. Already, the blending of different forecasting sources has been shown to provide enhanced precipitation (Xie and Arkin, 1996), temperature (Salazar et al., 2011) and wind speed (Xiao et al., 2015) forecasts. WOLFF2016197 For renewable energies in general, model blending has been identified as a great possible avenue for improving forecasting accuracy for both wind velocity (Tascikaraoglu and Uzunoglu, 2014) and solar radiation (Tuohy et al., 2015). The integration methods proposed across the literature mostly make use of statistical integration of data via linear regression (Lorenz et al., 2012) or other estimates. A weighting of models can drastically improve prediction as was pro posed in Kühnert (2016), whose results show that linear regression applied to numerical weather prediction (NWP) and cloud motion vector (CMV) models can improve the overall accuracy of forecasts on horizons from 0 to 5 h. The system described in Haupt et al. (2018) blends several short term forecasting models by weighting the model contributions according to their historical performance at each lead time.

Machine learning is a very popular approach to forecasting and time series in general, and it has seen some use in solar forecasting with ever

* Corresponding author.

growing popularity (Mellit, 2008; Voyant et al., 2017; Zamo et al., 2014a; Zamo et al., 2014b). Previous work shows the potential of using machine learning to combine NWP forecasts. For example, artificial neural networks (ANNs) can be applied as proposed by Voyant et al. (2012), where a NWP and meteorological current measurements are merged by means of an ANN. In another approach (Lu et al., 2015), three different NWPs are used to forecast meteorological variables, from which predictor variables are obtained and they are blended with random forest to predict day ahead radiation. The results again show that this combination is more accurate than the individual NWPs. Wolff et al. (2016) combines irradiance measurements, satellite and NWP to produce better forecasts of PV production using support vector machines (SVM) with notable results. The work of Aguiar et al. (2016) builds an ANN where ground measurements, European Center for Medium Range Weather Forecasts (ECMWF) and satellite data are blended. The experimental results show a clear increase of skill when multiple information sources are used. Machine learning and integration have been also used in operational environments (Hamann, 2017) with multiple configurations of input NWP models, learning algorithms and data size. Recently, Dersch et al. (2019) have proposed and evaluated an optimal combination of forecasting models specifically designed for obtaining improved DNI forecasts.

The models proposed across the literature have shown promising results for forecasting integration. The interest of the present work is to study the integration of different forecasting models in order to obtain improved short term (i.e. six hours ahead, and time resolution of 15 min) GHI and DNI radiation predictions. With this aim, we propose and evaluate different blending approaches that integrate the predictions of GHI (or DNI) provided by the four models analyzed in the companion paper (Part 1). The blending of those four models is of particular interest because they follow four almost independent approaches/foundations.

Two different blending approaches are studied and evaluated, namely: horizon and general approach. The difference between them is that the horizon approach constructs one model per forecasting horizon using training data from that horizon only, while the general approach constructs a single model trained with data from all forecasting horizons. The horizon approach trains models specialized on each horizon but there is less data to train each of the models, while the general one constructs a model independent of the horizon, being trained using data from all horizons. Both approaches make use of the SVM (Cortes and Vapnik, 1995). SVM models use as input the four models presented and assessed in Part 1, which will be referred hereinafter as the four predictors. SVM has been trained using linear and non linear kernels with the aim to study whether non linear blending is more adequate than linear.

Blending strategies may include additional parameters, beyond the models input. For instance, Lu et al. (2015) have proposed a novel methodology for model's blending that takes into account additional weather state parameters for day ahead solar radiation forecasting. These parameters accounted for different weather categories in which the different models provided enhanced performances. Results showed improved accuracy compared to reference model blending approaches. In McCandless et al. (2016b) and McCandless et al. (2016a) a cloud regime dependent short term statistical model is proposed, which also showed enhanced performance. In the companion paper (Part 1) weather conditions were found to have an important influence on the performance of the four models evaluated. Then, a specific study, that attempts to include the weather conditions in the model blending procedure, is here conducted. To this end, the weather types identified as relevant for the solar radiation in the study area (Rodríguez Benítez et al., 2018), and already assessed in the companion paper, are the starting point.

Finally, accurate solar forecasts at site (station) level are relevant for plant owners. On the other hand, regional average (or aggregated) forecasts for entire regions are important for transmission system operators (TSOs) (Pierro et al., 2017). As solar energy increases its share in electricity systems, an enhanced accuracy of the solar radiation forecast at grid level is needed in order to manage the electricity systems (Renné, 2014). In this work a specific blended regional model is presented and evaluated.

This work is organized as follows. 2 presents in detail the different blending approaches (horizon, general, weather type aware and regional forecast), including at the end of this section a brief introduction to the SVM methodology. In 3 the data and experimental procedure are introduced, while in 4 results are presented and discussed. Overall conclusions are provided in 5. Additional analyses are discussed in Appendices A and B.

2. Blending approaches

This section describes the methodology followed for obtaining the blending models. Firstly, two different blending strategies (general and by horizons) are explained. Secondly, an approach that constructs blended models conditioned to the weather types described in Rodríguez Benítez et al. (2018) will be presented. The previously mentioned blending approaches are suitable for individual stations. Therefore, in the third subsection, regional blending approaches are described. In principle, any machine learning technique could be used for obtaining the blending models. In this article, SVMs have been used because they have shown very good performance. Therefore, finally, a short description of the SVM for regression will be provided.

2.1. Horizon and general approaches

The approach to predict both types of irradiance (GHI and DNI) is to blend the four predictors described in the companion paper (Part 1) by means of machine learning models. The blending aims to find a function (f) that combines the predictors (P_i) using Eq. (1):

$$I = f(P_1, P_2, P_3, P_4) \tag{1}$$

where f is constructed using SVMs. To test the linearity of this problem, both linear and non linear SVM kernels have been used.

The blending approach aims to calculate at a given point in time (t) an accurate prediction of irradiance (I) for different forecasting horizons (h), from 15 min to 6 h, with 15 min steps. Two different approaches have been used to optimize the combination of the four predictors. The main difference between them is that the horizon approach constructs a model for each horizon, while the general approach trains a unique model valid for all horizons. Both are described below.

Horizon approach: This approach trains a different model f_h for each horizon, hence allowing for horizon dependent predictor blending. Therefore, there is a model for horizon 15, another for horizon 30, and so on, up to horizon 360 (thus, there are 24 models in total). Fig. 1 displays how each model f_h is trained using data belonging to horizon h only. Data for training model f_h is made of patterns like $((P_1(t, h), P_2(t, h), P_3(t, h), P_4(t, h)), I(t + h)$, for all t. The $P_i(t, h)$ denote predictors issued at time t, that make forecasts for time $t + h$. Once the models have been constructed, Eq. (2) shows how the f_h models can be used for irradiance forecasting. For instance, if at time t we would like to know the forecast in 15 min time, f_{15} would be used and $f_{15}(P_1(t, 15), P_2(t, 15), P_3(t, 15), P_4(t, 15))$ would be computed.

$$I\left(t + h\right) = \begin{cases} f_{15}(P_1(t, 15), P_2(t, 15), P_3(t, 15), P_4(t, 15)) & \text{if } h = 15 \\ f_{30}(P_1(t, 30), P_2(t, 30), P_3(t, 30), P_4(t, 30)) & \text{if } h = 30 \\ \cdots \\ f_{360}(P_1(t, 360), P_2(t, 360), P_3(t, 360), P_4(t, 360)) & \text{if } h = 360 \end{cases} \tag{2}$$

General approach: This approach constructs a single model f that blends the four predictors independently of the horizon. Fig. 2 shows how data from all horizons is combined and a single model f is trained. In this case, training data are the patterns

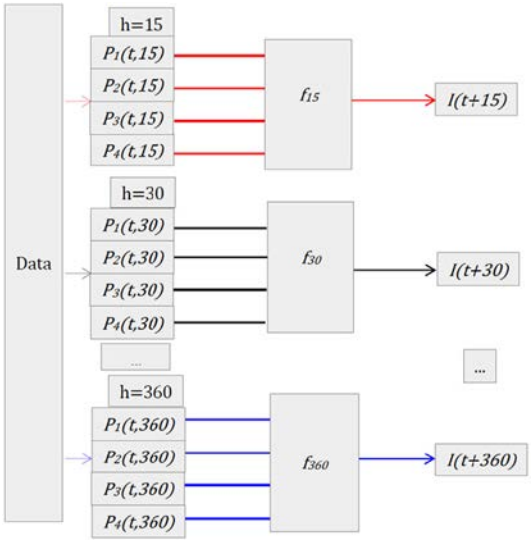

Fig. 1. Horizon Blending Approach: there is one model f_h per forecast horizon. Each f_h is trained with data belonging to that horizon. In order to make predictions for $I(t+h)$, the appropriate model f_h and predictors $P_i(t,h)$ are used.

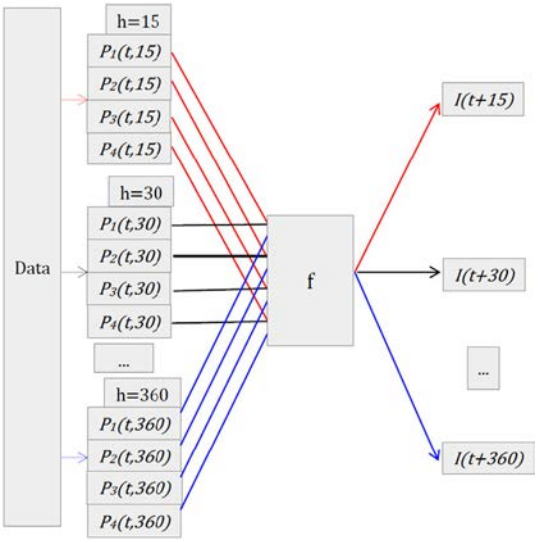

Fig. 2. General Approach: there is a single model f valid for all horizons, which is trained with data belonging to all horizons. In order to make predictions for $I(t+h)$, the appropriate predictors $P_i(t,h)$ are used together with model f.

$(P_1(t,h), P_2(t,h), P_3(t,h), P_4(t,h))$, $I(t+h)$, for all available t and h. Once the model f is trained, it is used for irradiance prediction using Eq. (3). It can be noticed that, although $P_i(t,h)$ is used as input for predictions at $t+h$, f itself is independent of h.

$$I(t+h) = f(P_1(t,h), P_2(t,h), P_3(t,h), P_4(t,h)) \tag{3}$$

2.2. Blending approach using weather types

In the companion paper (Part 1), a remarkable dependence of the four predictors on the weather conditions was found (Section 5.4). Motivated by this result, a specific blending analysis depending on the weather conditions is undertaken. The same weather types (WT) described in Section 5.4 of the companion paper have been used. There are basically four weather types: synoptic perturbation over the study area (WT1), transient weather conditions (WT2), moderate high pressure anomalies over the study area (WT3), and high pressure system over the whole study area (WT4). The aim is to construct blended models specialized in each of these weather types.

With this purpose, the general blending approach described in Section 2.1 has been modified to consider WT's. For this analysis, four different general models have been trained grouping data by the four WT's considered. Each of those four models is constructed using the scheme shown in Fig. 2, that is joining data for all horizons but separating data by WT. Therefore, in this case, there will be four general blending models, one per WT. The horizon approach could also have been used, but it has not been considered because it would involve dividing the data into too many groups (one group for each WT and horizon), resulting in 4 WT's × 24 horizons = 96 models (versus the four models required by the general approach). This implies that there would be few data for training each of the models. That is the main reason why the general approach has been used instead.

2.3. Regional forecasting

Regional forecasting means that only the regional average (or aggregated) irradiance is of interest, instead of the local irradiance prediction addressed in previous sections. In principle, regional forecasting should be more accurate, as local fluctuations will be averaged. The aim is to predict the average of irradiance (GHI and DNI) over a region, which in this case, it will be the mean of the four individual stations (Jaen, Lisbon, Madrid, and Seville).

In this work, two different regional blending approaches are studied to predict irradiance at the different forecasting horizons considered. The first one performs regional forecasting by computing the average of the four local blending models. That is, if Eq. (4) represents the blending model for station S (where S can be Jaen, Lisbon, Madrid, and Seville), then the regional model is given by Eq. (5), where r is the number of stations ($r = 4$ in this case).

$$I^S(t+h) = f^S(P_1^S(t,h), P_2^S(t,h), P_3^S(t,h), P_4^S(t,h)) \tag{4}$$

$$\bar{I}\left(t+h\right) = \frac{1}{r}\sum_{S=1}^{r} f^S(P_1^S(t,h), P_2^S(t,h), P_3^S(t,h), P_4^S(t,h)) \tag{5}$$

The second one constructs a model (Eq. (6)) whose inputs are the four available predictors at each of the r stations. Therefore, r stations x 4 predictors will be used as inputs. The target output to train model f is now directly the average of irradiance (GHI or DNI) at the four locations.

$$\bar{I}(t+h) = f(P_1^{S_1}(t,h),\ldots,P_4^{S_1}(t,h),\ldots,P_1^{S_r}(t,h),\ldots,P_4^{S_r}(t,h)) \tag{6}$$

2.4. Support Vector Machines

SVM (Cortes and Vapnik, 1995) is a machine learning algorithm often used for classification and regression problems. For classification, the learning algorithm searches the optimal hyperplane dividing two different classes. This is achieved maximizing the margin between the instances of both classes. Non linear models can be obtained by means of kernel functions (the so called kernel trick). These functions transform data into a higher dimensional space where the maximum margin hyperplane is computed.

In this article, SVM's have been used for regression. The SVM approach to regression has been described in Scholkopf and Smola (2001), and some details will be provided here. Assume a training data set $\{(x_1, y_1), \ldots, (x_n, y_n)\}$ where the outputs y_i are real values, and the x_i are the input variables. The equation $f(x) = \langle w, x\rangle + b$ is the general form of the model, where $\langle\cdot,\cdot\rangle$ is the dot product, b a real number and w is the weights vector, to be optimized. The objective is to look for a model f as simple as possible, but achieving predictions for all instances with errors no larger than some allowed deviation ε. This can be done by minimizing the modulus of w by means of the optimization problem represented in Eq. (7).

$$\text{minimize} \frac{1}{2}\left\|w\right\|^2$$

$$\text{subject} \{ y_i - \langle w, x_i \rangle - b \leqslant \varepsilon \langle w, x_i \rangle + b - y_i \leqslant \varepsilon \tag{7}$$

However, Eq. (7) assumes the existence of a valid solution that approximates all (x_i, y_i) pairs within the allowed deviation ε. This may not always be the case (for instance, if some of the instances are very noisy) and some minor errors should be allowed in order to find a feasible solution. This is achieved by introducing slack variables ξ_i and ξ_i^* (errors beyond the allowed deviation ε). The final optimization problem is presented in Eq. (8).

$$\text{minimize} \frac{1}{2}\left\|w\right\|^2 + C\sum_{i=1}^{n}(\xi_i + \xi_i^*)$$

$$\text{subject} \{ y_i - \langle w, x_i \rangle - b \leqslant \varepsilon + \xi_i \langle w, x_i \rangle + b - y_i \leqslant \varepsilon + \xi_i^* \xi_i, \xi_i^* \geqslant 0, \tag{8}$$

where $C > 0$ is a constant that determines the degree of importance of the two goals in the optimization process (the complexity of the model measured by $||w||^2$ and the size of the slack variables ξ_i and ξ_i^*. If C is too large, then the slack variables will be small, but this may lead to overfitting to noise. If C is too small, the optimization process will focus on minimizing the complexity of the model, and thus underfitting may be the result. C is therefore the main hyper parameter that must be tuned in order to obtain well performing SVM's. This optimization problem can be further extended to non linear models by means of the kernel trick, already mentioned for classification. Different kernels can be used (polynomial, radial, sigmoidal, …). One of the most widely used kernels is the gaussian (or radial) one. In that case, the SVM model becomes that of Eq. (9).

$$f(x) = \sum_{i=1}^{n}(\alpha_i - \alpha_i^*) e^{\frac{-||x-x_l||^2}{2\sigma^2}} \tag{9}$$

Those x_i in Eq. (9) for which $(\alpha_i - \alpha_i^*) \neq 0$ are the support vectors, that is, the training instances selected by the optimization method for constructing model f. $(\alpha_i - \alpha_i^*)$ are factors computed during optimization that determine the importance of each of the support vectors, and σ is the standard deviation of the gaussian function, around each of the support vectors.

In order to train SVM models, the e1071 library (Meyer et al., 2019) for R language (R Core Team, 2019) has been used. The Caret library (Kuhn, 2008; Kuhn et al., 2019) has also been used to facilitate tasks such as hyper parameter tuning.

3. Data and experimental methodology

The four predictors described in the companion paper (Part 1), namely Satellite, WRF Solar, Smart Persistence and CIADCast, are here used as inputs for the blending approaches. Also, the same forecasts dataset (Table 1 of Part 1) is here used for both training and evaluating the proposed blended models. Note that there is significantly less data as the horizon increases, due to the time range and the increasing time window from t to $t + h$. Forecasts are made at different time horizons, from 15 min to 6 h, with 15 min steps. Models are evaluated independently for the GHI and the DNI at the four evaluation stations: Seville, Jaen, Madrid and Lisbon.

Every approach described in 2 requires models to be trained and validated. In this work, cross validation (CV) has been applied for this purpose. CV is a common practice in machine learning validation. CV creates N random partitions (or folds) of the same size. For each partition i, a model is trained with all partitions but i, and tested on i. The CV result is the average of the i testing partitions.

Standard CV partitions the dataset randomly. This is appropriate when instances are independent but in the case of time series, there is a temporal dependency between instances. However, this kind of CV risks using consecutive days for both training and testing, which may result in overly optimistic estimations of performance. In order to mitigate this problem, a variation of CV has been used here (called grouped CV). There will be 4 different partitions (CV with $N = 4$), one for each week of every month. Therefore, partition 1 contains the first week of January, the first of February, and so on. This is similar for partition 2, with the second week of every month. This guarantees that, at least, training and testing partitions will never contain instances belonging to the same week.

The SVM method used for blending in this article can employ both linear and non linear kernels. In addition to the linear kernel, we have tested three non linear kernels (radial, polynomial, and sigmoidal). Appendix A contains the experimental comparison of these three kernels. The best performing non linear kernel is the radial one, and it has been used for the rest of experiments in this article. SVMs require tuning hyper parameter C (see Eq. (8)). This has been done by systematically evaluating different C values ($C = 0.25,0.5,1,2,4$) by means of standard CV on the training partition. It must be noted that the test partition is not used for hyper parameter tuning.

To measure the quality of the blending models, the metrics relative root mean square error (rRMSE), relative mean absolute error (rMAE), and RMSE forecast skill (FS_{RMSE}) presented in the companion paper (Part 1) have also been used.

4. Results and discussion

4.1. Overall performance of the Horizon and General approaches

In this section, we show the empirical results of the Horizon and General blending approaches described in Section 2.1 for the four stations: Jaen, Lisbon, Madrid, and Seville. Both approaches have been estimated using SVM with linear and radial kernels, resulting in four blending models, referred to as: SVMLinear Horizon, SVMRadial Horizon, SVMLinear General, and SVMRadial General. They are compared to the performance of the four original predictors. Both GHI and DNI are considered. The average errors (rRMSE and rMAE) for all horizons and for each station (Jaen, Lisbon, Madrid, Seville) are shown in Tables 1 and 2 for GHI and DNI, respectively.

As is observed in Table 1 (top), the average rRMSE for GHI of the four predictors is consistently higher than any of the blending approaches. The improvement attained using the blending models, compared to the best performing predictor model, is maximum at Lisbon. At this station the rRMSE of the best predictor is 49.97% and SVMLinear Horizon model value is 41.38%, i.e., about 9% absolute improvement, or 17% relative improvement. Jaen and Seville stations show a similar relative improvement (17% and 16%, respectively). Comparing blending techniques, it is observed that the rRMSE for different approaches is very similar, although the SVMLinear Horizon performs best in Jaen (28.83%), Lisbon (41.38%) and Madrid (32.20%). In Seville the lowest rRMSE of 27.23% is reached using the General approach and Linear SVM, although the differences in terms of rRMSE are very small. With respect to rMAE (Table 1 (bottom)), blending models also outperform the four predictors. In this case all stations show around 3% of absolute improvement. The maximum relative improvement is achieved at Jaen (14%) and Seville (15%). The best blending approach is SVMRadial General for all stations: Jaen (16.75%), Lisbon (29.02%), Madrid (20.12%) and Seville (15.92%). It is also observed that there is some variability across stations, errors in Lisbon tend to be higher than others while the error in Seville tends to be the lower than the rest. Regarding the standard deviation, the Lisbon station has the highest deviations in terms of rRMSE and rMAE. Furthermore, deviations of rRMSE and rMAE appear to be slightly higher for predictors than blending models, with the exception of WRF Solar, which shows the smallest deviations. In general terms it can be said that for GHI, on the one hand all blending approaches show a smaller error than any of

Table 1
Summary of average and standard deviation GHI results: (top) rRMSE and (bottom) rMAE. Over the line the four predictors and below the line the four blending approaches. The average is computed over all forecasting horizons. Values are in %.

	rRMSE			
	Jaen	Lisbon	Madrid	Seville
Satellite	35.85 (4.42)	49.97 (10.29)	39.53 (4.47)	33.64 (6.18)
WRF-Solar	35.35 (2.38)	51.11 (8.7)	36.3 (2.95)	32.37 (2.61)
SmartPersistance	34.87 (4.47)	50.1 (11.65)	38.7 (4.48)	34.23 (4.63)
CIADCast	35.36 (3.69)	50.76 (11.65)	41.61 (5.64)	33.82 (5.02)
SVMRadial General	29.19 (3.37)	41.94 (9.58)	32.89 (4.17)	27.67 (3.85)
SVMLinear General	28.98 (3.61)	41.67 (9.72)	32.33 (4.18)	**27.23** (3.73)
SVMRadial Horizon	28.97 (3.43)	42.31 (9.22)	32.5 (3.92)	27.86 (3.85)
SVMLinear Horizon	**28.83** (3.74)	**41.38** (10.4)	**32.2** (4.26)	27.28 (3.69)
	rMAE			
	Jaen	Lisbon	Madrid	Seville
Satellite	22.63 (3.35)	36.86 (8.66)	27.18 (3.45)	20.49 (4.29)
WRF-Solar	21.93 (2.14)	33.95 (7.62)	23.78 (2.58)	18.75 (1.75)
SmartPersistance	19.5 (3.91)	32.88 (10.34)	23.23 (4.37)	18.86 (3.66)
CIADCast	22.78 (2.83)	36.86 (10.18)	29.68 (4.47)	21.23 (3.87)
SVMRadial General	**16.75** (3.01)	**29.02** (8.38)	**20.12** (3.5)	**15.92** (3.1)
SVMLinear General	17.4 (2.91)	29.43 (8.45)	20.85 (3.54)	16.55 (2.86)
SVMRadial Horizon	17.64 (3.15)	30.35 (8.96)	20.79 (3.66)	17.08 (3.05)
SVMLinear Horizon	17.34 (3.21)	29.51 (10.06)	20.8 (3.89)	16.43 (3.1)

the predictors, while on the other hand, the standard deviation of the blending models is never larger than the maximum deviation of the four predictors. That is, better performance is not bought at the cost of in creasing variance.

A similar performance is observed for DNI forecasting (see Table 2). All error metrics are lower for the blending methods than the four predictors, and comparing the machine learning methods also shows that they perform similarly. The main difference between GHI and DNI is that the errors are overall much worse than for GHI (for example, rRMSE from Lisbon goes from 41.38% to 73.45% and rMAE goes from 29.02% to 50.51%). For rRMSE, the best approach appears to be the Horizon one. For Jaen (44.24%) and Lisbon (73.45%) the Radial SVM performs best, and for Madrid (55.48%) and Seville (41.81%) the Linear SVM has the lowest error. The improvement attained using the blending models, compared to the best performing input predictors, is maximum at Lisbon, about 14% of absolute improvement and 16% relative improvement. With respect to rMAE and DNI (Table 2 (bottom)), the average results show that the SVMRadial General ap proach outperforms all other models, as was also observed for GHI (see Table 1). The most important improvement versus the performance of predictors, is observed at the Lisbon station (about 7% in absolute value and 12% in relative value). In this case the maximum relative im provement happens at Seville station (14%). Standard deviation are in general larger than those of GHI (Table 1), but they follow a similar

Table 2
As in Table 1 but for the DNI.

	rRMSE			
	Jaen	Lisbon	Madrid	Seville
Satellite	53.36 (7.29)	88.99 (20.51)	66.69 (8.94)	51.35 (9.97)
WRFsolar	54.36 (2.99)	89.21 (22.5)	67.86 (4.03)	48.72 (3.17)
SmartPersistence	52.49 (9.81)	87.41 (27.48)	62.6 (11.16)	51.56 (9.08)
CIADCast	55.21 (7.71)	90.95 (25.49)	70.73 (10.05)	54.46 (10.28)
svmRadial General	45.15 (8.47)	73.99 (24.66)	56.19 (10.17)	42.54 (7.07)
svmLinear General	46.79 (6.76)	78.35 (21.26)	57.04 (9.97)	42.8 (6.54)
svmRadial Horizontes	**44.42** (6.05)	**73.45** (20.22)	55.75 (8.84)	42.08 (6.04)
svmLinear Horizontes	44.78 (7.18)	74.5 (21.41)	**55.48** (9.87)	**41.81** (7.03)
	rMAE			
	Jaen	Lisbon	Madrid	Seville
Satellite	36.25 (5.68)	67.96 (16.5)	46.53 (6.47)	34.74 (8.09)
WRFsolar	36.64 (2.82)	63.33 (17.69)	46.18 (3.69)	32.48 (2.78)
SmartPersistence	29.74 (8.16)	57.14 (22.99)	37.35 (9.36)	29.14 (7.5)
CIADCast	38.24 (5.57)	69.17 (21.55)	50.99 (8.2)	37.37 (8.43)
svmRadial General	**27.09** (6.99)	**50.51** (20.51)	**35.5** (8.34)	**25.14** (6.17)
svmLinear General	28.9 (5.83)	55.05 (17.06)	36.54 (8.33)	27.41 (5.42)
svmRadial Horizontes	27.52 (7)	51.43 (20.9)	36.27 (8.7)	25.97 (6.23)
svmLinear Horizontes	28.55 (6.53)	54.76 (18.77)	36.33 (9.06)	27.15 (6.03)

Table 3
Average FS_{RMSE} for GHI and DNI of the four blending approaches. The average is computed over all forecasting horizons. Values are in %.

	GHI FS_{RMSE}			
	Jaen	Lisbon	Madrid	Seville
SVMRadial General	16.19 (0.74)	16.21 (0.97)	15.04 (0.78)	19.14 (1.05)
SVMLinear General	16.89 (1.53)	16.72 (1.42)	16.51 (0.97)	20.48 (1.21)
SVMRadial Horizon	16.86 (1.67)	15.79 (1.02)	16.09 (1.44)	18.52 (1.6)
SVMLinear Horizon	17.17 (2.11)	17.18 (1.53)	16.74 (1.11)	20.33 (2.17)
	DNI FS_{RMSE}			
	Jaen	Lisbon	Madrid	Seville
SVMRadial General	13.33 (0.71)	14.46 (0.47)	10.19 (0.41)	17.09 (1.37)
SVMLinear General	10.76 (3.79)	10.39 (2.95)	8.87 (0.87)	16.79 (2.82)
SVMRadial Horizon	14.93 (4.87)	15.26 (4.24)	10.89 (2.96)	18.21 (3.26)
SVMLinear Horizon	13.81 (2.62)	13.49 (2.45)	10.88 (1.17)	18.38 (1.59)

pattern except that Satellite display smaller deviation than blending models in general. Similarly to GHI, also for DNI the standard deviation of the blending models is never large than the maximum of the predictors, therefore better performance is not bought at the cost of increasing variance.

Additionally, in Table 3 the average of the forecast skill (FS_{RMSE}) for all horizons and each location is shown. The FS_{RMSE} is calculated for both GHI and DNI for the four blending approaches. It is observed that the blending approaches achieve good values of FS_{RMSE} for GHI and DNI, being better for GHI. As it has been observed previously concerning RMSE, there are no important differences regarding the performance of the four different blending models, although Horizon models tend to perform better in general.

4.2. Horizon and General approaches performance depending on the forecasting horizon

Here, the performance of the blending approaches and the four predictors is broken down by forecasting horizon for GHI and DNI and for the four stations. Given that machine learning methods outperform the four predictors, in the following figures the line named "optimal" represents the best performance for each horizon among the four predictors (Satellite, WRF Solar, Smart Persistence and CIADCast), in terms of minimum rRMSE or rMAE. Note that this reference is highly stringent, since the best performing predictor at each forecasting horizon is unknown beforehand.

Fig. 3 displays the rRMSE for GHI along the horizons for the four stations. It is observed that the blending approaches outperform the optimal line for all forecasting horizons. Blending machine learning models reach relative improvements with respect to the optimal line of 6% in the worst case and 18% in the best one. On the other hand, the errors of the blending machine learning models overlap with each other, it being difficult to decide the best one approach for every horizon. However, SVMLinear Horizon approach seems to perform better than the other approaches at least in some horizons. This is true for all stations, except for Seville, where this approach performs similar to SVMGeneral Linear model. In any case, the difference in terms of rRMSE is very small. The rRMSE in every station increases with the horizon, without large differences between blending models.

In Fig. 4 the evolution of the rMAE for GHI is shown. In all stations, the optimal line is also worse than any other model, except at some horizons in Lisbon (from 330 to 360) and in Seville (from 285 to 345), where the optimal line is similar to the SVMRadial Horizon approach. For rMAE, the relative improvement of blending models with respect to the optimal line goes from 3% (worst case) to 18% (best case, Jaen around 4 h lead time). With respect to blending approaches, the best model for all stations is the SVMRadial General approach. There is some overlap for some horizons with the SVMLinear Horizon approach and with the SVMLinear General approach in Lisbon station, but it still shows the best results. The relative improvement of the SVMRadial General model with respect to the SVMLinear Horizon approach is around 3%, 4% and 5% in many cases. It is also observed that the SVMRadial Horizon approach is very poor for rMAE metric. It ends up being outperformed by all other machine learning models at far horizons in Jaen (from $h = 285$ to $h = 360$) and Lisbon (from $h = 225$ to $h = 360$) and at most horizons for Seville station. For short horizons, all models start at the same range and the rMAE grows as the horizon increases, but the growth amount depends on the station.

Unlike the rRMSE, observing the rMAE values for GHI, there is a clear best model for all stations, the SVMRadial General approach. It is better for Jaen, Madrid and Seville than the rest of the machine learning approaches, and it is similar to the SVMLinear General and SVMLinear Horizon approaches for the Lisbon station.

Fig. 5 shows the rRMSE for DNI forecasting along the horizons. Similarly to GHI forecasting, the blending approaches outperform the optimal line, with relative improvements between 5% and 16%. There is also overlap between blending machine learning models, but as the horizon increases, the SVMLinear Horizon approach outperforms other models, where relative improvements of 2%, 3% and 4% are reached with respect to other approaches. At short horizons, the SVMRadial Horizon model is slightly better, but the improvements are smaller. This pattern repeats for all stations, but it is more noticeable in Jaen, Madrid and Seville. Here the SVMLinear General model is worse than the other models by a fair margin mainly for long horizons.

Fig. 6 shows the rMAE evolution for DNI forecasts. Unlike every other result presented before, here the optimal line outperforms or is similar to the blending models at short horizons (up to 60 min). As the

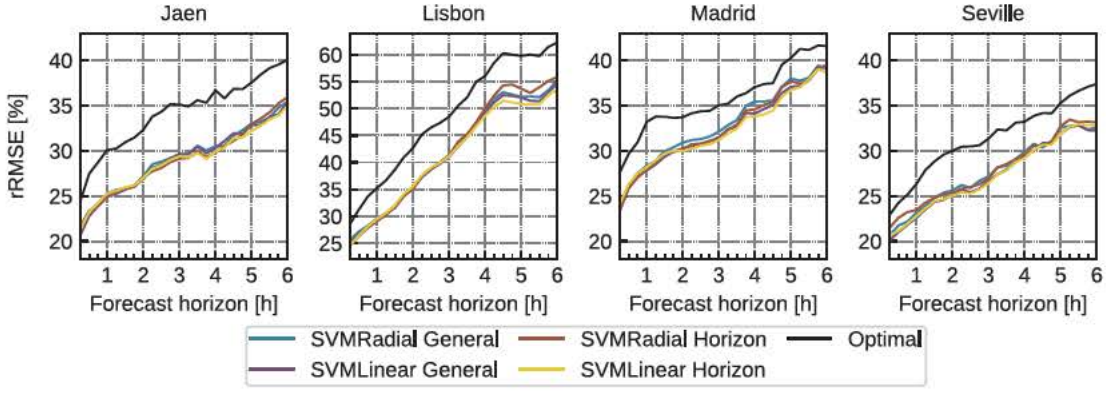

Fig. 3. GHI rRMSE of blending models (General and Horizon) by horizon. "Optimal" displays the best performance out of the four predictors (the optimal line). Note the difference range of values for the Lisbon station.

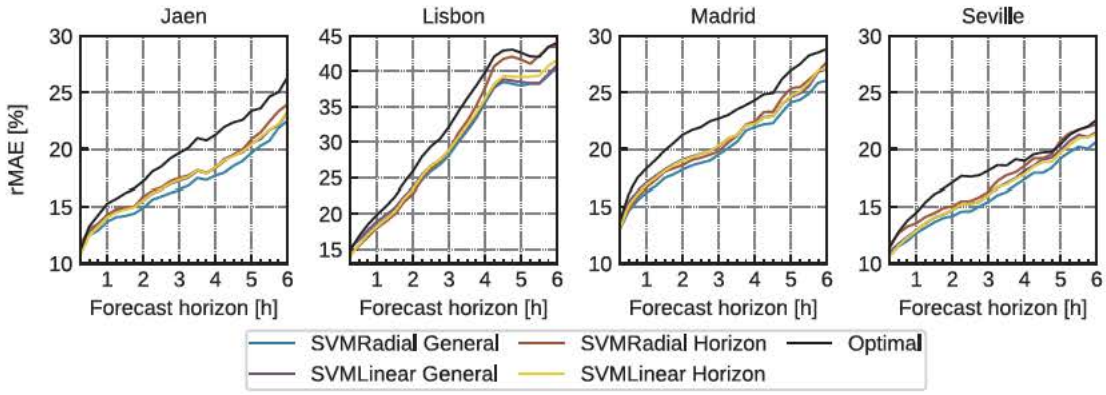

Fig. 4. As in Fig. 3 but for the GHI rMAE forecasting errors.

horizon increases, the differences become greater and the SVMRadial General approach appears to offer the best performance for long term predictions, between 3% and 16% relative improvement over the optimal line. It is also observed that this approach overlaps with the SVMRadial Horizon model in some stations and for short horizons. However, as the horizon increases, the advantage of the SVMRadial General blending model becomes clearer, obtaining relative improvements up to 8%.

In summary, for GHI the four blending models perform similarly with respect to rRMSE, although for some horizons SVMLinear Horizon is slightly better. For DNI and rRMSE, the SVMRadial Horizon model seems the best model for short horizons and the SVMLinear Horizon one for far horizons. For rMAE the SVMRadial General model is the best for both GHI and DNI, although for DNI this shows more clearly at far horizons. Overall, the blending approaches outperform the optimal line for most of the forecasting horizons, at all stations and for both metrics, rRMSE and rMAE, reaching relative improvements from 3% to 18%.

It can also be seen that the differences between the optimal DNI line and blending models increases with the forecasting horizon. Therefore, it can be concluded that the main added value of the blended model is attained at the end of the forecasting horizon and that the improvement statistics summarized in Table 2 can mainly be attributed to the longest forecasting horizons. For the case of the GHI, the differences among forecasting horizons are not so relevant, and the blending models provide a similar improvement along the whole forecasting period.

Comparisons of the improvements of the forecasting error attained here by model blending with those obtained in similar work are difficult due to, particularly, the differences in the dataset (location climatology, input models, and length of the dataset). A reference work is Wolff et al. (2016), that proposed and evaluated an optimal linear combination of three GHI short term forecasting models (persistence, satellite, and NWP). Evaluation was conducted in Germany for the period March to November. Model combination provided the lowest errors for all lead times, with improvements of a few percent of the installed solar power capacity. More recently, Dersch et al. (2019) evaluated an optimal combination of five DNI short term forecasting models (two satellite derived, two NWP derived and persistence). Evaluation was conducted in two stations located in south eastern Spain and northern Africa. Results showed that the blended model outperformed all individual models for lead times below 300 min, in terms of rRMSE, when NWP models were the best performing models. Maximum relative improvements were found to be around 20% for one hour lead time, but differences rapidly decreased with lead time. Results here presented are qualitatively similar, although climatology is more stringent here, regarding solar radiation forecasting, for the analyzed stations.

In addition to the above analysis for rRMSE and rMAE, a study of forecasting skill (FS_{RMSE}) broken down by horizon is provided in Appendix B, where the blending models dependence on the sky conditions (using the clearness index, k_t) is analyzed.

4.3. Analysis of models performance depending on the synoptic conditions

The role of the weather conditions on model blending is here assessed, based on the four WTs described in Rodríguez Benítez et al. (2018). As has been mentioned in Section 2.2, only the general approach has been used to study the influence of WTs in the blending model. Linear and non linear approximations have been validated, but results are only displayed for the linear one (referred to as SVMLinear WT) because it showed a better performance.

Fig. 7 breaks down SVMLinear WT performance (rRMSE) by forecasting horizon, for both GHI and DNI. Performance is compared with the other blending approaches (General and Horizon) for the four stations. Results show that the inclusion of the weather types in the blending provides a relatively modest, but significant, improvement of the forecasts accuracy compared to the other blending approaches for some stations at certain forecasting horizons. Particularly, the

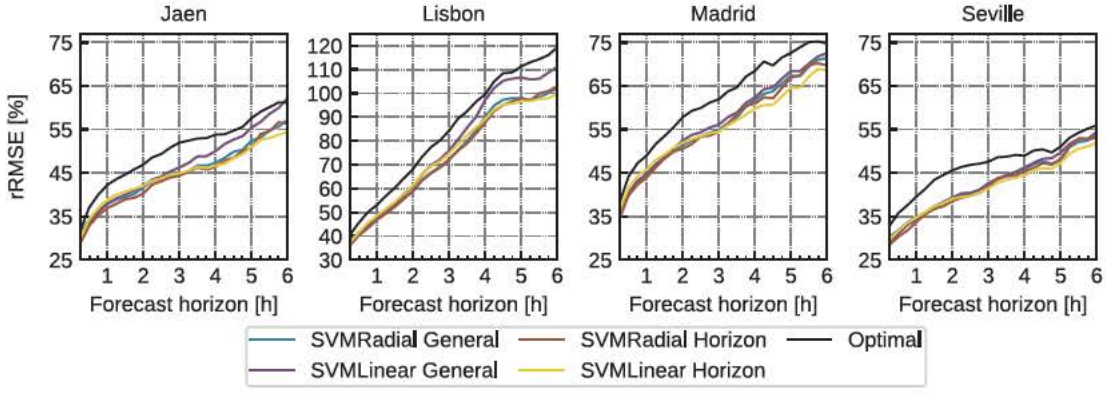

Fig. 5. As in Fig. 3 but for DNI rRMSE forecasting errors.

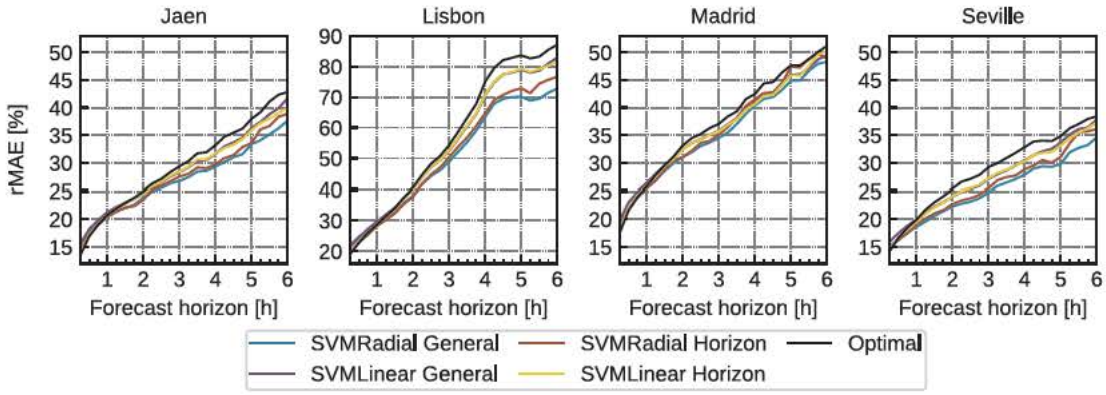

Fig. 6. As in Fig. 5 but for DNI rMAE forecasting errors.

SVMLinear WT is shown to be the most accurate model for GHI at Seville for horizons larger than four hours, aproximately. The relative improvement is about 3% at the end of the forecasting period compared with SVMLinear Horizon (overall the best approach for rRMSE). For the DNI and Jaen, the SVMLinear WT shows better forecast for time horizons below 3 h. But the best performance is observed for DNI and Seville, where a relative improvement between 1% and 3% is found for time horizons between 1 and 3 h (compared to SVMRadial Horizon, overall the best approach for rRMSE for short horizons). On the other hand, weather type information does not improve the forecast for Lisbon and Madrid.

The use of WT in model blending regarding short term solar radiation forecasting has not received much attention in the literature. Lu et al. (2015) reported an absolute improvement of the forecasting errors of about 30% (in terms of RMSE) when using a model blending approach based of WTs. But comparison is difficult due to, mainly, the different input predictors (they only used different NWP models as input of the blending approach) and the forecasting horizon (they assessed day ahead forecast).

4.4. Regional model approach

Next, experimental results for the two regional approaches described in Section 2.3 are presented. In this case, SVM with radial kernel and a general approach (a single model for all horizons) have been used to construct the two regional blending models. They are referred to as SVMRadial General Mean (the first one: mean of local SVMRadial General models) and SVMRadial General Regional (the second one: a model constructed with all available predictors of all local stations). Other approaches (General Linear, Horizon Linear or Horizon with Radial Kernel) might have been used, but only the general non linear one has been selected here for empirical validation because it has shown good performance overall.

The results for both approaches are shown in Fig. 8, where the metrics (rRMSE and rMAE) have been calculated at each horizon and for both GHI and DNI. For comparison purposes, the figure also includes, for each predictor, its mean over the four locations. For instance, CIADCast in Fig. 8 is the mean of the CIADCast predictor over Jaen, Seville, Madrid, and Lisbon.

As may be expected, regional forecasts derived from each predictor (Satellite, WRF Solar, Smart Persistence and CIADCast) show considerably smaller errors than forecasts of single stations (Figs. 3 6), because of the spatial decorrelation of the forecasts errors. The Smart Persistence predictor performance is particularly outstanding, since only WRF Solar, for GHI and for lead times greater than 4 h, is competitive. It is also observed that both regional blending approaches

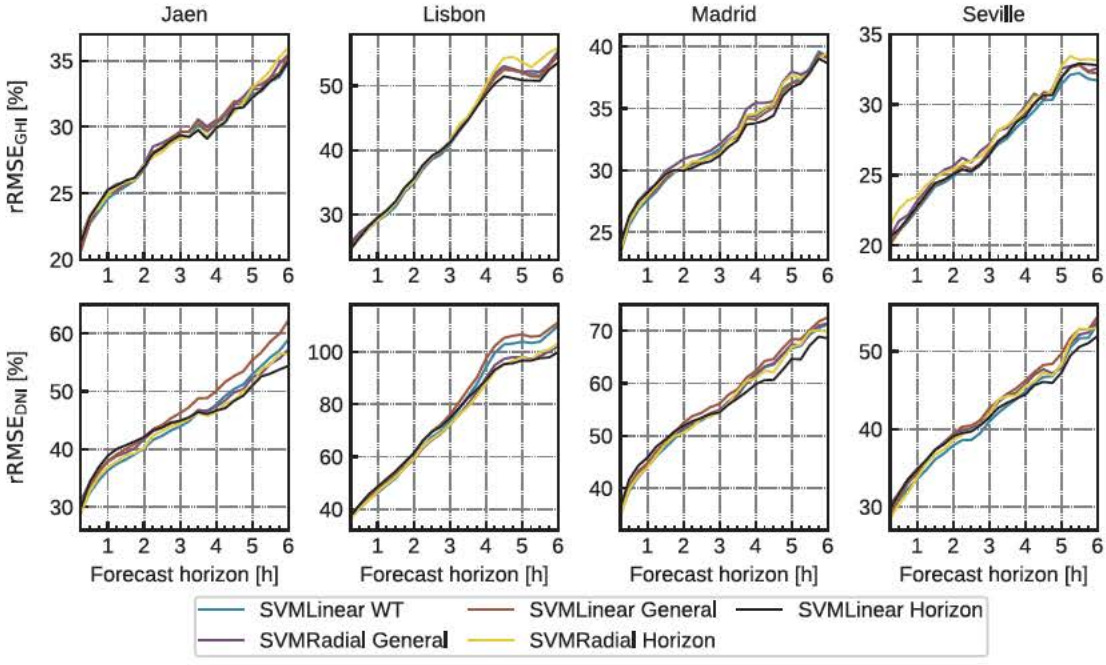

Fig. 7. Performance of SVMLinear-WT model for rRMSE (GHI and DNI) compared with Global and Horizon approaches in all stations.

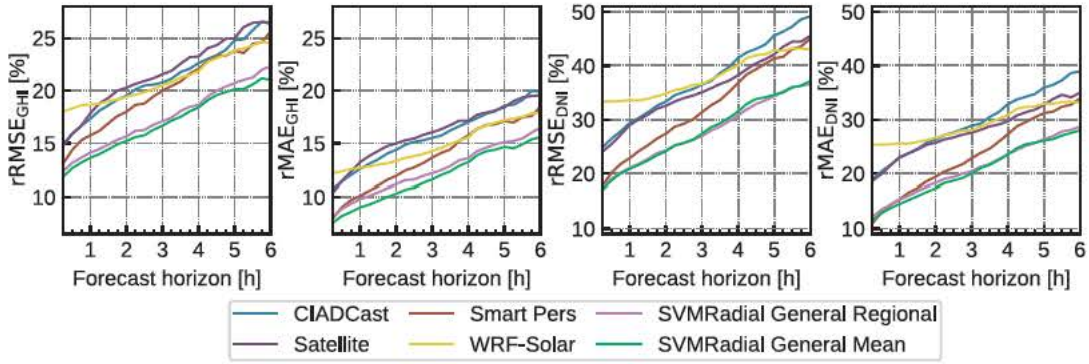

Fig. 8. Performance of the two machine learning regional blending models (SVMRadial-General-Regional and SVMRadial-General-Mean). As reference, the performance of the four forecasting predictors (Satellite, WRF-Solar, Smart Persistence and CIADCast) and their average (mean) are also shown. Values are displayed both for the GHI and DNI and for rRMSE and rMAE metrics. The range of error values (in %) are different for GHI and DNI.

Table 4
Summary for average GHI errors and standard deviation of the four predictors means (top) and the two regional blending approaches (bottom). The average is computed over all forecasting horizons. Values are in %.

	rMAE	rRMSE
Satellite	16.06 (2.5)	21.76 (3.33)
WRFsolar	14.83 (1.91)	21.10 (2.15)
SmartPersistence	13.78 (2.99)	20.03 (3.47)
CIADCast	15.89 (2.63)	21.43 (3.23)
SVMRadial-General-Mean	**11.87** (2.42)	**16.94** (2.8)
SVMRadial-General-Regional	12.51 (2.35)	17.48 (2.09)

Table 5
As in Table 4 but for the DNI

	rMAE	rRMSE
Satellite	27.87 (4.54)	35.64 (6.04)
WRFsolar	29.09 (3.02)	37.78 (3.74)
SmartPersistence	23.44 (6.71)	32.29 (7.92)
CIADCast	30.00 (5.71)	38.03 (7)
SVMRadial-General-Mean	**20.57** (4.98)	28.01 (6.01)
SVMRadial-General-Regional	21.05 (4.81)	**27.84** (5.79)

display similar performance and they outperform the predictors for all horizons and for both GHI and DNI. Error reduction attained with these approaches increases with the forecast horizon (Fig. 8), and is higher for rRMSE than for rMAE. For instance, an absolute improvement of about 8% is observed for DNI and rRMSE at the end of the forecast period, when comparing the blending model against the best performing one (WRF Solar).

As a summary of the regional forecast results, Table 4 (GHI) and Table 5 (DNI) show the average rRMSE and rMAE for all horizons and evaluated regional models. It can be seen that, indeed, the two regional approaches are very close, but SVMRadial General Mean displays smaller errors (except for rRMSE DNI). The relative improvement in rRMSE obtained by model blending is about 15% for GHI and 13% for DNI, compared to the best performing input predictor. In rMAE, the improvements are 14% (GHI) and 12% (DNI). Comparing Tables 1,2 with 4 and 5, it is observed, both for GHI and DNI, that the rRMSE values of the regional forecast are about one half of those of the individual stations. Previous work (Wolff et al., 2016) has reported that GHI forecast errors of regional forecasts are reduced to about one third of the single stations forecasts. Differences may be explained based on the number of stations involved in the analysis, here only 4. This limited number of stations, only accounts for part of the spatial variability of the errors, and does not allow a full evaluation of the compensation effects of the forecasting error associated with the spatial decorrelation of these errors. Particularly, a further reduction of the error can be anticipated if the number of stations analyzed in the study area would be greater. Regarding DNI, no previous work has assessed regional DNI forecasts.

5. Summary and Conclusions

In this article, the integration of GHI and DNI forecasting models has been addressed, with the aim of improving the prediction accuracies of those models used individually. This is achieved by using the forecasting models as predictors and blending them by means of machine learning techniques. In particular, in this work, the four forecasting models analyzed in the companion article (Satellite based

Table 6
Summary of rRMSE for the non-linear kernels: (top) GHI and (bottom) DNI. The average is computed over all forecasting horizons. Values are in %.

	rRMSE GHI			
Kernel	Jaen	Lisbon	Madrid	Seville
Radial	**16.75**	**29.02**	**20.12**	**15.92**
Polynomic	18.13	30.87	21.66	17.84
Sigmoidal	24.12	39.10	30.09	23.27
	rRMSE DNI			
Kernel	Jaen	Lisbon	Madrid	Seville
Radial	**27.09**	**50.51**	**35.5**	**25.14**
Polynomic	29.41	56.45	37.57	29.43
Sigmoidal	51.83	85.25	67.33	51.32

Table 7
Summary of MAE for the non-linear kernels: (top) GHI and (bottom) DNI. The average is computed over all forecasting horizons. Values are in %.

	rMAE GHI			
Kernel	Jaen	Lisbon	Madrid	Seville
Radial	**29.19**	**41.94**	**32.89**	**27.67**
Polynomic	30.36	42.46	34.05	29.40
Sigmoidal	39.43	49.25	45.89	37.60
	rMAE DNI			
Kernel	Jaen	Lisbon	Madrid	Seville
Radial	**45.15**	**73.99**	**56.19**	**42.54**
Polynomic	46.83	78.86	57.65	45.81
Sigmoidal	72.68	92.52	84.88	70.58

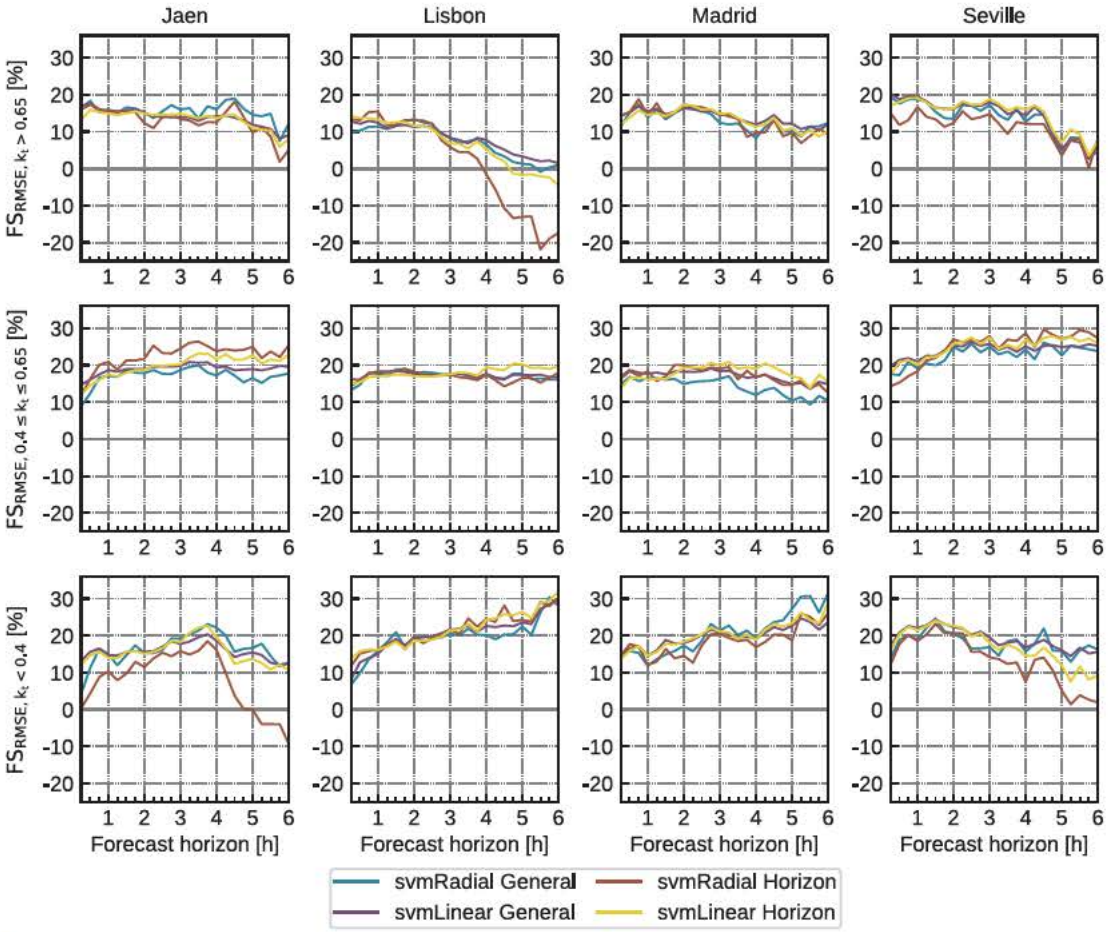

Fig. 9. FS_{RMSE} of the blending models (General and Horizon) for GHI according to daily mean k_t. Top row: $k_t > 0{:}65$ (clear sky), Middle row: $0{:}4 <= kt <= 0{:}65$ (partly cloudy), Bottom row: $kt < 0{:}4$ (overcast conditions). Values are in %.

model, WRF Solar, Smart Persistence and CIADCast) are blended using SVM's. Two approaches have been evaluated: Horizon and General. The first one constructs a model for each horizon and the second one trains a single model valid for all horizons.

The blending approaches have been validated at four locations (Jaen, Lisbon, Madrid, and Seville) for forecasting horizons from 15 min to 6 h with steps of 15 min. The two commonly used SVM kernels (linear and radial) have been tested. Results show that all blending approaches are able to reduce significantly the error of the original four predictors. This occurs for both GHI and DNI, for all horizons, and locations, and the two evaluation metrics. In general, it is observed that the improvement provided by the blending approaches does not strongly depend on the forecasting horizon, except for DNI. In that case, the improvement tends to increase for long horizons.

Differences between the blending approaches themselves are small, although the best approach depends on the kind of error to be used: Horizon models work slightly better for reducing rRMSE, while the General non linear (radial) model works better for rMAE (being that difference larger than for rRMSE). This is true for both GHI and DNI.

With regard to the blending approach that uses weather type information, it has been shown that there can be some improvement depending on the location. In this study, knowledge about weather conditions is useful for GHI at Seville for horizons larger than four hours. For DNI the gain is obtained for Seville and Jaen for horizons

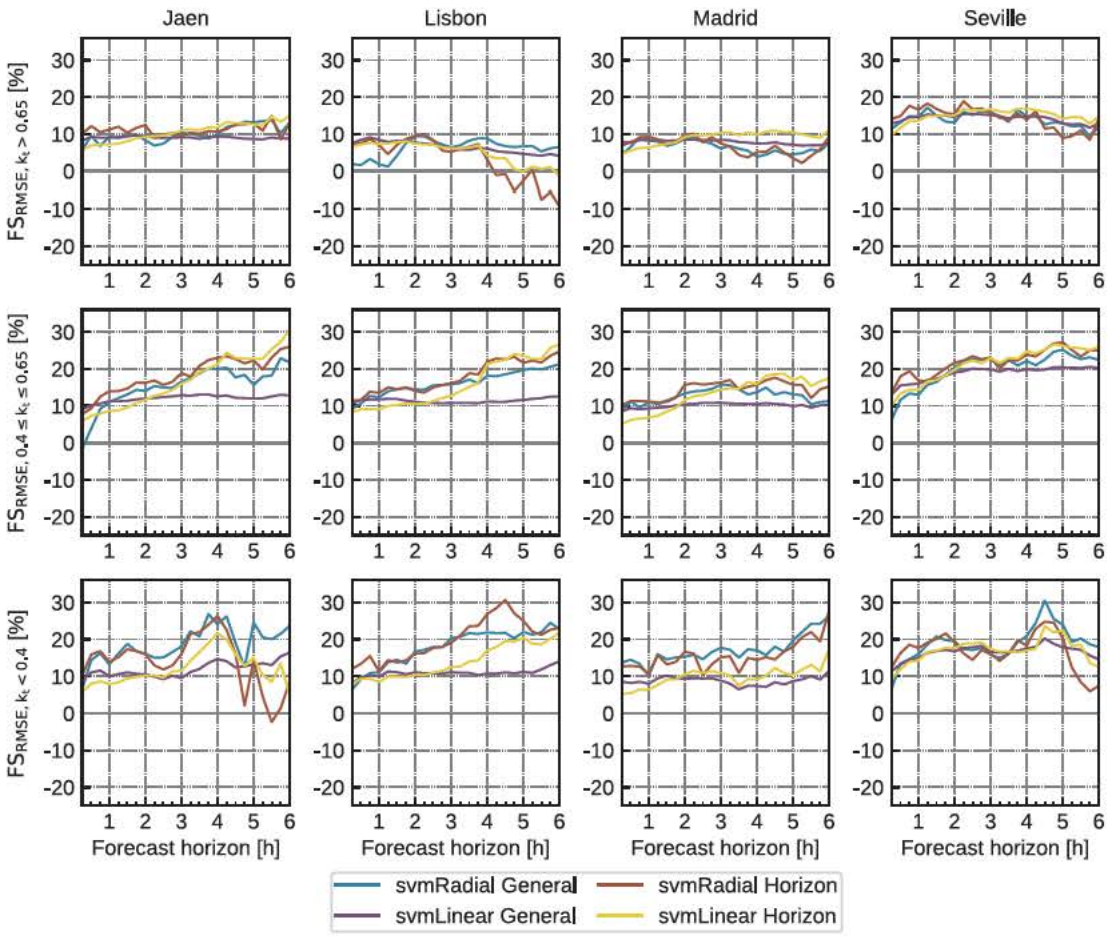

Fig. 10. FS_{RMSE} of the blending models (General and Horizon) for DNI according to daily mean k_t. Top row: $k_t > 0{:}\ 65$ (clear sky), Middle row: $0{:}\ 4 <= kt <= 0{:}\ 65$ (partly cloudy), Bottom row: $kt < 0{:}\ 4$ (overcast conditions). Values are in %.

below three hours. Improvements occur only for rRMSE. This is prob ably due to weather type help predicting outliers better, which is more important for the rRMSE metric.

Finally, predictor blending has also been applied in a regional context, where the aim is to predict the mean radiation of several lo cations in the region of interest. In this work, the region is represented by the four locations studied. Two machine learning approaches have been analyzed: the mean of the local blending models, and a model that uses as inputs all available predictors at all locations. Regional fore casting using the individual predictors (by computing their mean over the four locations) has been used for comparison. Again, the two re gional blending methods outperform the regional predictors. This conclusion is general for both GHI and DNI, all horizons, and both metrics. The differences between the two approaches are small, al though the first one obtains the smallest errors.

Declaration of Competing Interest

The authors declared that there is no conflict of interest.

Acknowledgements

The authors are supported by the Spanish Ministry of Economy and Competitiveness, projects ENE2014 56126 C2 1 R and ENE2014 56126 C2 2 R (http://prosol.uc3m.es). The University of Jan team are also supported by FEDER funds and by the Junta de Andalucia (Research group TEP 220). The authors are in debt with the National Centers for Environmental Prediction (NCEP), EUMETSAT, Faculdade de Ciencias da Universidade de Lisboa, Grupo de Energa Solar of the Universidad Politcnica de Madrid and Abengoa Solar for providing the data used in this work.

Appendix A. Experimental comparison of non-linear SVM kernels

The aim of this Appendix is to carry out an experimental comparison of the performance of different non linear SVM kernels: radial, polynomial (with degree 3), and sigmoidal. This study has been done using the general blending approach for both rRMSE and rMAE, for both GHI and DNI, and for the four stations (Jaen, Lisbon, Madrid, and Seville). Results are shown in Tables 6,7. The errors represent the average over all the forecasting horizons. It is observed that in all cases the radial kernel obtains the smallest errors. The polynomial kernel shows similar performance to the radial one, while the sigmoidal errors much larger.

Appendix B. Analysis of blending models skill broken down by daily mean clearness index (k_t)

Figs. 9 and 10 show the forecast skill (FS_{RMSE}) of the blending models, according to the daily mean clearness index (k_t) observed when the forecasts were issued, for GHI and DNI, respectively. The performance has been broken down on days of high, medium, and low irradiance, which correspond with $k_t > 0{:}\ 65$ (clear sky), $0{:}\ 4 \leqslant kt \leqslant 0{:}\ 65$ (partly cloudy), and $kt < 0{:}\ 4$ (overcast conditions), respectively. As in Part I, we follow

(Lara Fanego et al., 2012) to classify days: those with mean (kt) greater than 0.65 are considered as clear sky conditions, between 0.4 and 0.65 partly cloudy, and below 0.4 as overcast conditions.

For both GHI and DNI it can be seen that for all stations, for all sky conditions, for all horizons and for most blending models, the FS_{RMSE} is above zero. That means they perform better than persistence in all cases. The only exception is the SVMRadial Horizon model, that in some cases for long horizons the FS_{RMSE} is below zero (for both GHI and DNI in Jaen/overcast and Lisbon/clear sky). It is also observed that blending models perform similarly in most situations. The exceptions are, for GHI (Fig. 9), the already mentioned SVMRadial Horizon model displays a different behavior to the rest. For DNI (Fig. 10), in addition to the SVMRadial Horizon model, the SVMLinear General also displays worse trends for partly cloudy skies and for overcast conditions, model behavior is less similar in general.

Figs. 9 and 10 also show that blending models are sensitive to the sky conditions. In particular for GHI, it can be seen that for clear sky days, FS_{RMSE} tends to decrease with the horizon, for all stations and models. This is presumably due to persistence performing well in that kind of days. For partly cloudy days, FS_{RMSE} tends to slightly increase in the first horizons and keep stable for longer horizons (except in Madrid where a slight decrease is observed). For overcast conditions, FS_{RMSE} either increases with horizon (Lisbon and Madrid) or starts increasing but decreases at some horizon (Jaen and Seville). For DNI, models also display sensitivity to sky conditions although the behavior is different to the one observed for GHI. In this case, for clear sky the FS_{RMSE} is mostly stable across horizons, and for partly cloudy the skill tends to increase with horizon. For overcast conditions, there is a tendency to initially increase and eventually decrease, however, there is a larger variability in the behavior of the different models, therefore a general characterization is difficult to state.

References

Aguiar, L.M., Pereira, B., Lauret, P., Díaz, F., David, M., 2016. Combining solar irradiance measurements, satellite-derived data and a numerical weather prediction model to improve intra-day solar forecasting. Renewable Energy 97, 599–610. https://doi.org/10.1016/j.renene.2016.06.018.. http://www.sciencedirect.com/science/article/pii/S0960148116305390.

Cortes, C., Vapnik, V., 1995. Support-vector networks. Machine Learn. 20, 273–297. https://doi.org/10.1007/BF00994018.

Dersch, J., Schroedter-Homscheidt, M., Gairaa, K., Hanrieder, N., Landelius, T., Lindskog, M., Müller, S., Ramirez Santigosa, L., Sirch, T., Wilbert, S., 2019. Impact of DNI nowcasting on annual revenues of CSP plants for a time of delivery based feed in tariff. Meteorologische Zeitschrift, – doi:https://doi.org/10.1127/metz/2019/0925.

Hamann, H.F., 2017. A Multi-scale, Multi-Model, Machine-Learning Solar Forecasting Technology, https://doi.org/10.2172/1395344.

Haupt, S.E., Kosović, B., Jensen, T., Lazo, J.K., Lee, J.A., Jiménez, P.A., Cowie, J., Wiener, G., McCandless, T.C., Rogers, M., Miller, S., Sengupta, M., Xie, Y., Hinkelman, L., Kalb, P., Heiser, J., 2018. Building the Sun4Cast System: Improvements in Solar Power Forecasting. Bull. Am. Meteorol. Soc. 99, 121–136. doi:https://doi.org/10.1175/BAMS-D-16-0221.1.

Kuhn, M., 2008. Building predictive models in r using the caret package. J. Stat. Softw., Articles 28, 1–26. https://doi.org/10.18637/jss.v028.i05.. https://www.jstatsoft.org/v028/i05.

Kuhn, M., Wing, J., Weston, S., Williams, A., Keefer, C., Engelhardt, A., Cooper, T., Mayer, Z., Kenkel, B., Benesty, M., Lescarbeau, R., Ziem, A., Scrucca, L., Tang, Y., Candan, C., Hunt., T., 2019. caret: Classification and Regression Training. https://CRAN.R-project.org/package=caret. r package version 6.0-84.

Kühnert, J., 2016. Development of a photovoltaic power prediction system for forecast horizons of several hours. Ph.D. thesis. Carl von Ossietzky Universität, Oldenburg.

Lara-Fanego, V., Ruiz-Arias, J., Pozo-Vázquez, D., Santos-Alamillos, F., Tovar-Pescador, J., 2012. Evaluation of the wrf model solar irradiance forecasts in andalusia (southern spain). Sol. Energy 86, 2200–2217.

Lorenz, E., Kühnert, J., Heinemann, D., 2012. Short term forecasting of solar irradiance by combining satellite data and numerical weather predictions. In: 27th European Photovoltaic Solar Energy Conference and Exhibition, pp. 4401–4405. https://www.eupvsec-proceedings.com/proceedings?paper=20627, doi:https://doi.org/10.4229/27thEUPVSection2012-6DO.12.1.

Lu, S., Hwang, Y., Khabibrakhmanov, I., Marianno, F.J., Shao, X., Zhang, J., Hodge, B.M., Hamann, H.F., 2015. Machine learning based multi-physical-model blending for enhancing renewable energy forecast-improvement via situation dependent error correction. In: 2015 European control conference (ECC), IEEE, pp. 283–290.

Lu, S., Hwang, Youngdeok, Khabibrakhmanov, I., Marianno, F.J., Shao, Xiaoyan, Zhang, J., Hodge, B., Hamann, H.F., 2015. Machine learning based multi-physical-model blending for enhancing renewable energy forecast - improvement via situation dependent error correction. In: 2015 European Control Conference (ECC), pp. 283–290. https://doi.org/10.1109/ECC.2015.7330558.

McCandless, T., Haupt, S., Young, G., 2016a. A regime-dependent artificial neural network technique for short-range solar irradiance forecasting. Renewable Energy 89, 351–359. https://doi.org/10.1016/j.renene.2015.12.030.. http://www.sciencedirect.com/science/article/pii/S0960148115305346.

McCandless, T.C., Young, G.S., Haupt, S.E., Hinkelman, L.M., 2016b. Regime-Dependent Short-Range Solar Irradiance Forecasting. Journal of Applied Meteorology and Climatology 55, 1599–1613. doi:https://doi.org/10.1175/JAMC-D-15-0354.1.

Mellit, A., 2008. Artificial Intelligence technique for modelling and forecasting of solar radiation data: a review. Int. J. Artif. Intell. Soft Comput. 1, 52–76. https://doi.org/10.1504/IJAISC.2008.021264.. https://www.inderscience.com/info/inarticle.php?artid=21264.

Meyer, D., Dimitriadou, E., Hornik, K., Weingessel, A., Leisch, F., 2019. e1071: Misc Functions of the Department of Statistics, Probability Theory Group (Formerly: E1071), TU Wien. https://CRAN.R-project.org/package=e1071. r package version 1.7-2.

Pierro, M., Felice, M.D., Maggioni, E., Moser, D., Perotto, A., Spada, F., Cornaro, C., 2017. Data-driven upscaling methods for regional photovoltaic power estimation and forecast using satellite and numerical weather prediction data. Sol. Energy 158, 1026–1038. https://doi.org/10.1016/j.solener.2017.09.068.. http://www.sciencedirect.com/science/article/pii/S0038092X17308617.

R Core Team, 2019. R: A Language and Environment for Statistical Computing. R Foundation for Statistical Computing, Vienna, Austria. https://www.R-project.org/.

Renné, D.S., 2014. Emerging Meteorological Requirements to Support High Penetrations of Variable Renewable Energy Sources: Solar Energy. Springer, New York, New York, NY, pp. 257–273.

Rodríguez-Benítez, F.J., Arbizu-Barrena, C., Santos-Alamillos, F.J., Tovar-Pescador, J., Pozo-Vázquez, D., 2018. Analysis of the intra-day solar resource variability in the Iberian Peninsula. Sol. Energy 171, 374–387. https://doi.org/10.1016/j.solener.2018.06.060.. http://www.sciencedirect.com/science/article/pii/S0038092X18306108.

Salazar, E., Sansó, B., Finley, A.O., Hammerling, D., Steinsland, I., Wang, X., Delamater, P., 2011. Comparing and blending regional climate model predictions for the American Southwest. J. Agric. Biol. Environ. Stat. 16, 586–605. https://doi.org/10.1007/s13253-011-0074-6.

Scholkopf, B., Smola, A.J., 2001. Learning with Kernels: Support Vector Machines, Regularization, Optimization, and Beyond. MIT Press, Cambridge, MA, USA.

Tascikaraoglu, A., Uzunoglu, M., 2014. A review of combined approaches for prediction of short-term wind speed and power. Renew. Sustain. Energy Rev. 34, 243–254. https://doi.org/10.1016/j.rser.2014.03.033.. http://www.sciencedirect.com/science/article/pii/S1364032114001944.

Tuohy, A., Zack, J., Haupt, S.E., Sharp, J., Ahlstrom, M., Dise, S., Grimit, E., Mohrlen, C., Lange, M., Casado, M.G., Black, J., Marquis, M., Collier, C., 2015. Solar forecasting: methods, challenges, and performance. IEEE Power Energ. Mag. 13, 50–59. https://doi.org/10.1109/MPE.2015.2461351.

Vislocky, R.L., Fritsch, J.M., 1995. Improved model output and statistics through model consensus. Bull. Am. Meteorol. Soc. 76, 1157–1164. https://doi.org/10.1175/1520-0477(1995) 076<1157:IMOSFT>2.0.CO;2.

Voyant, C., Muselli, M., Paoli, C., Nivet, M.L., 2012. Numerical weather prediction (NWP) and hybrid ARMA/ANN model to predict global radiation. Energy 39, 341–355. http://www.sciencedirect.com/science/article/pii/S0360544212000114, doi:https://doi.org/10.1016/j.energy.2012.01.006. sustainable Energy and Environmental Protection 2010.

Voyant, C., Notton, G., Kalogirou, S., Nivet, M.L., Paoli, C., Motte, F., Fouilloy, A., 2017. Machine learning methods for solar radiation forecasting: A review. Renewable Energy 105, 569–582. https://doi.org/10.1016/j.renene.2016.12.095.. http://www.sciencedirect.com/science/article/pii/S0960148116311648.

Wolff, B., Kühnert, J., Lorenz, E., Kramer, O., Heinemann, D., 2016. Comparing support vector regression for PV power forecasting to a physical modeling approach using measurement, numerical weather prediction, and cloud motion data. Sol. Energy 135, 197–208. https://doi.org/10.1016/j.solener.2016.05.051.. http://www.sciencedirect.com/science/article/pii/S0038092X16301682.

Xiao, L., Wang, J., Dong, Y., Wu, J., 2015. Combined forecasting models for wind energy forecasting: A case study in China. Renew. Sustain. Energy Rev. 44, 271–288. https://doi.org/10.1016/j.rser.2014.12.012.. http://www.sciencedirect.com/science/article/pii/S1364032114010648.

Xie, P., Arkin, P.A., 1996. Analyses of Global Monthly Precipitation Using Gauge Observations, Satellite Estimates, and Numerical Model Predictions. J. Clim. 9, 840–858. https://doi.org/10.1175/1520-0442(1996) 009<0840:AOGMPU>2.0.CO;2.

Zamo, M., Mestre, O., Arbogast, P., Pannekoucke, O., 2014a. A benchmark of statistical regression methods for short-term forecasting of photovoltaic electricity production, part I: Deterministic forecast of hourly production. Sol. Energy 105, 792–803. https://doi.org/10.1016/j.solener.2013.12.006.. http://www.sciencedirect.com/science/article/pii/S0038092X13005239.

Zamo, M., Mestre, O., Arbogast, P., Pannekoucke, O., 2014b. A benchmark of statistical regression methods for short-term forecasting of photovoltaic electricity production. Part II: Probabilistic forecast of daily production. Sol. Energy 105, 804–816. https://doi.org/10.1016/j.solener.2014.03.026.. http://www.sciencedirect.com/science/article/pii/S0038092X14001601.